



Investigation of Complex Permittivity of XLPO Insulated Photovoltaic DC Cables Due to Thermal Aging

Ehtasham Mustafa^{1,2}, Ramy S. A. Afia^{2,3},
and Zoltán Ádám Tamus^{2(✉)}

¹ Department of Electrical Engineering, Gomal University,
Dera Ismail Khan, Pakistan

² Department of Electric Power Engineering,
Budapest University of Technology and Economics, Budapest, Hungary
{mustafa.ehtasham, tamus.adam}@vet.bme.hu

³ Department of Electric Power and Machines Engineering,
Helwan University, Cairo, Egypt
ramysaad@h-eng.helwan.edu.eg

Abstract. To study the effect of thermal aging on the low voltage DC cables used in photovoltaic systems, XLPO based cable samples were thermally aged for four different cycles of 240, 480, 720 and 960 h at 120 °C. This aging time was equivalent to 20, 40, 60 and 80 years of service period at 60 °C. The dielectric properties, real and imaginary part of permittivity were investigated for a frequency range of 20 Hz to 500 kHz using impedance analyzer. The polarization and leakage current effects have been discussed due to the thermal aging. The results show that the real part of permittivity increased with the aging due to the creation of dipoles because of the morphological changes happening inside the material. While the imaginary part of permittivity decreased at low frequencies and increased at higher frequencies. Also, there has been shifting of minimum value of imaginary part of permittivity to lower frequency, 500 Hz from 2 kHz with aging, showing that the resistance of the material increased at low frequency and the material becomes stiffer and hence an end-of-point to the degradation of insulation material has reached.

Keywords: Thermal aging · Photovoltaic systems cables · Dielectric property · XLPO

1 Introduction

The depletion of the naturally occurring energy sources and the effect of the carbon emission on the environment have made the use of renewable energy more important. They have the advantages of being clean, green and reusable. Photovoltaic (PV) system is one such renewable energy source out of other available sources, being considered safe and environment-friendly. On the other side, the reported number of faults occurring in the system has increased with an increase in its usage. The failure of the cable insulation in general and of DC cables in particular in one such failure. Since, the

DC cables are used in connecting the PV modules and inverters and are exposed to a number of stresses, i.e., ultraviolet radiation, heat, humidity, mechanical, electrical and thermal. As a result, the phenomenon of degradation, aging, in these cables is more as compared to other components of the PV systems.

Since the insulation of the cables is made of polymer, so the thermal stress which affects the structure of the polymer is considered to be more important than others. The thermal stress could be due to the Ohmic current or environmental temperature. Cross-linked polyolefin (XLPO) has been widely used polymer in PV insulation cables due to number of advantages such as thermal stability, dielectric properties, and solvent resistance. However, due to aging the chemical and physical properties of the XLPO will change under thermal stress and may affect the performance of the cable. The aging of insulation may result in leakage current which may increase with the passage of time and result in electric sparks and hence system failure. This makes the study of the real cause of aging of the insulation inevitable. A reliable condition monitoring (CM) technique helps in better understanding the aging of insulation. The CM techniques can be used to study either mechanical, chemical or electrical properties. The first two properties are studied by the destructive methods, while in recent times some non-destructive CM techniques have been reported to study the electrical properties of low voltage cables [1–7]. But none of them have been used to study the behavior of LV cables used in PV systems.

This paper has been aimed to study the dielectric properties; real (ϵ') and imaginary (ϵ'') part of permittivity of LV PV cables under the thermal stress. The method is useful in understanding the production of polarization and conduction losses due to the morphological changes happening inside the insulation due to the thermal stress. In this work, XLPO based LV PV DC cables were thermally aged at 120 °C for four cycles each of 10 days. The ϵ' and ϵ'' were studied using impedance analyzer for a frequency range of 20 Hz–500 kHz for each thermal cycle. The method was very helpful in studying the effect of thermal stress on the polarization and conduction losses in the insulation material, which makes the method capable of using it in PV systems as a potential CM technique.

2 Experimental Work

2.1 XLPO Based LV PV DC Cable

The cross-sectional view of LV XLPO based PV DC cable used for the study is shown in Fig. 1. XLPO has been used both as the primary insulation and the jacket of the cable. The XLPO is a semi-crystalline material which has a complex crystalline melting point [8]. Table 1 summarized different characteristics of the cable.

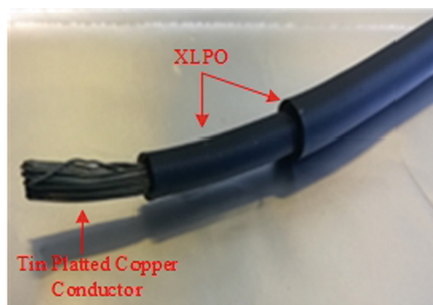


Fig. 1. XLPO based DC cable under investigation

Table 1. PV cable characteristics parameters.

Parameters	Values
Conductor	Tin plated copper conductor
Conductor diameter	2.25 mm
Outer insulation/Jacket	XLPO
Outer diameter	3.55 mm
Primary insulation	XLPO
Rated conductor temperature	-40 °C to 120 °C
Rated voltage	DC: 1.5 kV/AC: 1.0 kV

2.2 Accelerated Aging

A group of five cable samples, each one meter long, were subjected to thermal stress at 120 °C for four different oven aging periods of 240, 480, 720 and 960 h. These were equivalent to 20, 40, 60 and 80 years of service time at 60 °C, which were calculated using the Arrhenius model. The jacket and the insulation were kept in contact with the conductor to obtain the results as the cable is subjected to the field conditions. The samples were removed from the oven after each thermal cycle for the dielectric property analysis.

2.3 Measurement of Dielectric Properties

The measurement of dielectric properties was carried out using impedance analyzer for a frequency range of 20 Hz to 500 kHz at an applied voltage of 5 V_{rms} . The impedance of the cable was measured in R-C parallel configuration. The input signal terminal was connected to the conductor and the output signal terminal to a wire braid positioned on the outer surface of the cable. To reduce any pickup from the external noises, the cable samples along with the electrodes setup were placed in the Faraday cage. The

measurements were carried out at a temperature of $25\text{ }^{\circ}\text{C} \pm 2\%$. The real (ϵ') and imaginary (ϵ'') parts of the complex permittivity were calculated using the relationships [9]:

$$\epsilon' = \frac{dC}{A\epsilon_o} \tag{1}$$

$$\epsilon'' = \frac{d}{A\omega R\epsilon_o} \tag{2}$$

Where d and A are the thickness of the insulation and area of the electrode, respectively. The permittivity of vacuum shown as ϵ_o and ω is the angular frequency.

3 Experimental Results

The behavior of the real part (ϵ') and imaginary part (ϵ'') of permittivity are shown in Figs. 2 and 3 for a frequency range of 20 Hz to 500 kHz. The ϵ' increases as the frequency is decreased irrespective of the aging. After the first thermal cycle, ϵ' has decreased for all the frequencies. But an increase has been observed in ϵ' after the second and third thermal cycles. After the fourth cycle of thermal stress, a decrease in ϵ' at 20, 40 and 100 Hz has been observed while at all other frequencies it has increased.

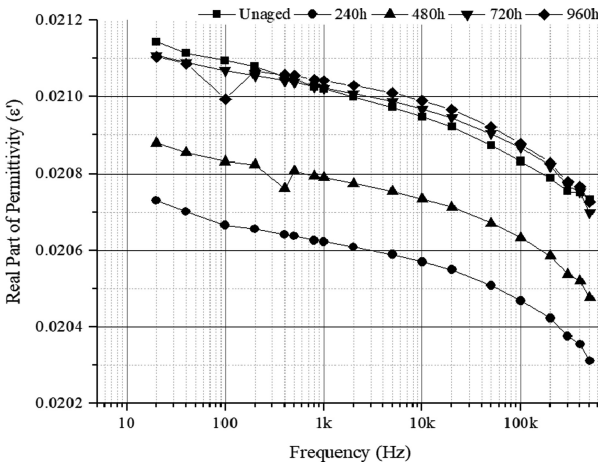


Fig. 2. Real part of permittivity (in a scale of 10^2) v/s frequency

For the ϵ'' the graph has been plotted between 400 Hz and 500 kHz, as at low frequencies below 400 Hz, the resistance of the jacket and insulation is higher than the

range of impedance analyzer. The ε'' have increased as the frequency is increased regardless of the aging. The effect of the first thermal cycle on ε'' has been a decrease in its value. While after the second thermal cycle, an increase has been observed between a frequency range of 400 Hz and 20 kHz. While at all other frequencies a decrease has been detected. After the third thermal cycle, a decrease in the values of ε'' has been noted at 200 Hz and at the frequency range of 800 Hz and 5 kHz, while at all other frequencies, an increase has been observed. At the end of the fourth thermal cycle stress, there is an increase between 5 kHz and 500 kHz while a decrease has been observed at 400 Hz and 2 kHz.

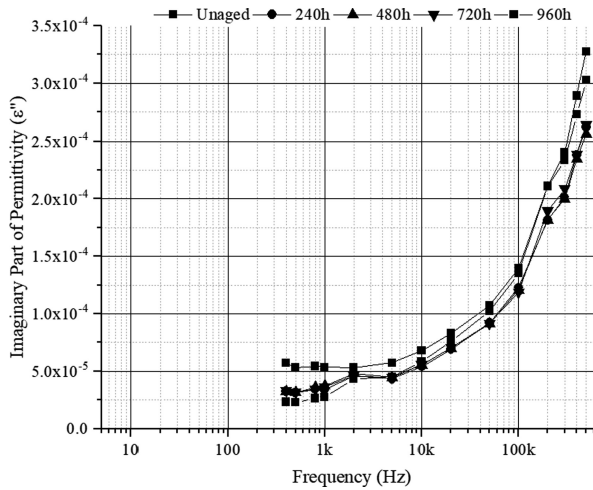


Fig. 3. Imaginary part of permittivity v/s frequency

For a better understanding of thermal stress effect on the jacket and insulation, reference frequencies have been selected to study the changing behavior of ε'' . Figure 4 shows the behavior of ε'' against the equivalent aging years at a reference frequency of 400 Hz, 500 Hz and 10 kHz. From the plot, it has been observed that at 400 Hz and 500 Hz there is decrease in the values of ε'' with aging while an increase has been observed at a higher frequency, 10 kHz.

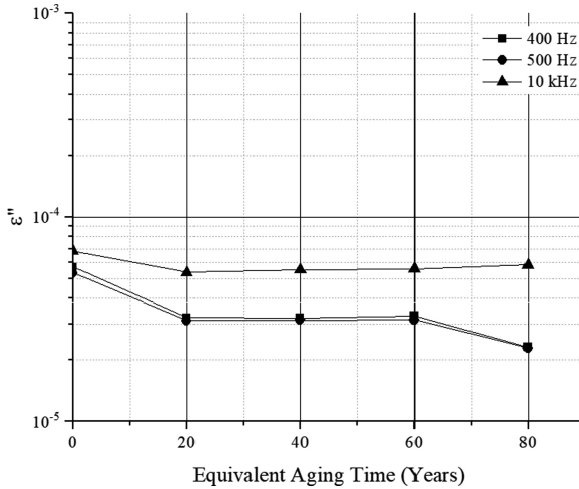


Fig. 4. Behavior of imaginary part of permittivity at 400 Hz, 500 Hz, and 10 kHz

4 Discussion

Since the dipole orientation has a great contribution to the real part of permittivity as the insulation material used in cables are polar in nature. The general profile of the real permittivity with the change to frequency can be attributed as the increase in frequency restricts the dipole orientation. The initial decrease in the ϵ' values after the first thermal cycle can be due to the moisture evaporation as the water is naturally polar. But the increase after each cycle, can be recognized due to the structural changes in the insulation material which resulted in the creation of dipoles. While the decrease at low frequencies 20, 40 and 100 Hz shows that at the low frequencies the dipoles contributing to polarization have decreased due to more structural changes happening in the material due to thermals stress.

The imaginary part of permittivity, ϵ'' is related to the leakage current loss or the conductivity of the material. The decrease of ϵ'' after the first thermal cycle, indicates the evaporation of the moisture, as a result, the charges contributing to conduction are restricted. While an increase of ϵ'' in the frequency range between 400 Hz and 20 kHz after the second thermal cycle shows that due to the structural changes happening inside the material, the charged particles are contributing to the leakage current. The increase of ϵ'' at higher frequencies after the third thermal cycle, 10 kHz to 500 kHz shows that the charge carriers present at higher frequencies have been created since at the second thermal cycle at this range of frequency ϵ'' decreased. This trend shows that the thermal stress has strongly effected the structure of the XLPO. This change has been shown as at lower frequency range, 400 Hz to 5 kHz, where the ϵ'' values have decreased. This means that inside the material new bonds have been created and the material resistance has increased resulting in the decrease of charge carriers. The fourth thermal cycle has a more profound effect on the structure of XLPO, as more increase in the value of ϵ'' at higher frequency has been noted while at low frequency the decrease

in the values is more. This shows that XLPO has become stiffer with aging, as a result at low frequency there are less charge carriers.

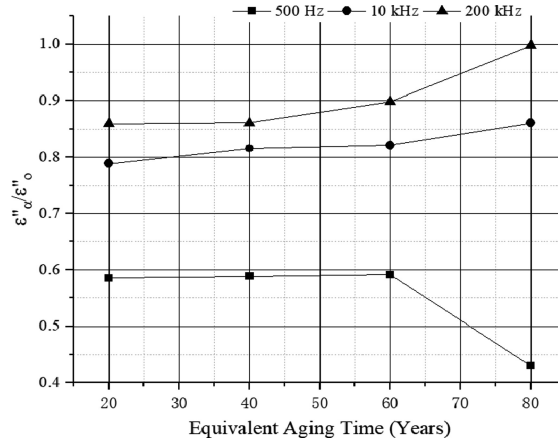


Fig. 5. Variation of the imaginary part of permittivity with aging

The change of ϵ'' at lower and higher frequencies has been studied by plotting the graph of ϵ'' versus equivalent aging time (years) for three frequencies i.e., 500 Hz, 10 kHz and 200 kHz, Fig. 5. As discussed earlier at a lower frequency, 500 Hz, the ϵ'' has decreased with aging while at higher frequencies, 10 kHz and 200 kHz it has increased. The structural changes happening in XLPO due to the thermal aging have resulted in more conduction charges in the high frequency range.

The shifting of minimum values of ϵ'' to lower frequency from 2 kHz to 500 Hz with thermal aging is shown in Fig. 6. After shifting of the minimum value at 500 Hz at first thermal cycle, it remains at this frequency for the next three thermal cycles, which shows that the polar or ionic particles at low frequencies have decreased which were contributing to the conduction. The decrease in the values of ϵ'' at low frequencies and shifting of the minimum value to lower frequency shows that the phenomenon contributing to the alteration to the dielectric property of the insulation material have reached to either conclusion or stabilization after 40-80 years.

It should be noted that during the fabrication process of insulation material different inorganic compounds are added for different purposes such as anti-oxidants, plasticizers, flame retardants, and dyes. These contribute to the structural changes happening inside the material due to aging and hence may affect the conduction and polarization processes. Consequently, for a more in-depth understanding of the effect of thermal aging on the XLPO material a good chemical analysis (TGA, DSC, and OIT) will be helpful.

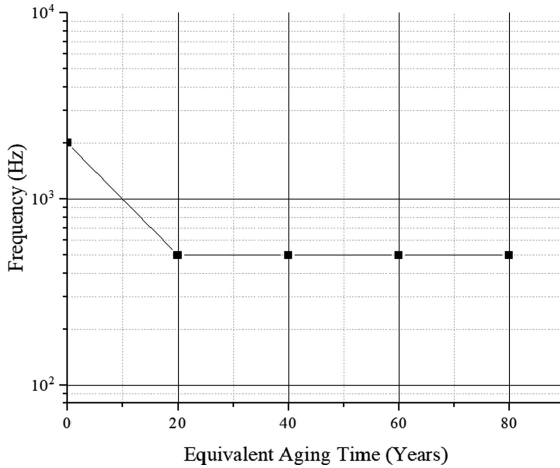


Fig. 6. Shifting of the imaginary part of permittivity to a lower frequency

5 Conclusion

The effect of thermal aging on the LV PV DC cables has been studied in this paper. The insulation material used in the cable was XLPO, semi-crystalline. The dielectric property, real and imaginary part of permittivity was used to study the effect of aging. The overall effect of thermal stress on XLPO has been an increase in the polarization effect, which is shown as an increase in ϵ' . While the ϵ'' showed a wide variation in its behavior with aging. At low frequencies the value of ϵ'' decreased with aging while at high frequencies it increased. This behavior suggests that morphological changes have happened inside the XLPO due to aging which are shown in the formation of dipoles, ϵ' and conduction charge particles, ϵ'' .

Besides, a shift in the minimum value of ϵ'' from the higher frequency of 2 kHz after first thermal cycle to 500 Hz and then being stable for next three cycles is an indication that the material has become stiffer and an end-of-point of insulation degradation has been reached. As a result, its resistance at low frequency has increased. A reliable chemical investigation technique will be helpful in better understanding the discussed dielectric behavior of XLPO.

References

1. Verardi, L., Fabiani, D., Montanari, G.C., Zak, P.: Electrical condition monitoring techniques for low-voltage cables used in nuclear power plants. In: 2013 IEEE Electrical Insulation Conference (EIC), pp. 504–508. IEEE, New York (2013)
2. Verardi, L., Fabiani, D., Montanari, G.C.: Electrical aging markers for EPR-based low-voltage cable insulation wiring of nuclear power plants. *Radiat. Phys. Chem.* **94**, 166–170 (2014)

3. Fantoni, P.F.: Condition monitoring of electrical cables using line resonance analysis (LIRA). In: 17th International Conference on Nuclear Engineering (ICONE), pp. 171–178. ASME (2009)
4. Asipuela, A., Mustafa, E., Afia, R.S.A., Tamus, Á.Z., Khan, M.Y.A.: Electrical condition monitoring of low voltage nuclear power plant cables: $\tan\delta$ and capacitance. In: IEEE 4th International Conference on Power Generation Systems and Renewable Energy Technologies (PGSRET), pp. 1–4. IEEE, New York (2018)
5. Mustafa, E., Tamus, Á.Z., Afia, R.S.A.: Thermal degradation and condition monitoring of low voltage power cables in nuclear power industry. *IFIP Advances in Information & Communication Technology*, vol. 553, pp. 405–413 (2019)
6. Csányi, M.G., Tamus, Á.Z., Iváncsy, T.: Investigation of central frequency and central loss factor values on dicotylphthalate (DOP) plasticized PVC films. In: 2018 IEEE International Conference on Diagnostics in Electrical Engineering (Diagnostika), pp. 1–4. IEEE, New York (2018)
7. Csányi, M.G., Tamus, Á.Z., Kordás, P.: Effect of enhancing distribution grid resilience on low voltage cable aging. *IFIP Advances in Information & Communication Technology*, vol. 521, pp. 300–307 (2018)
8. Celina, M.C., Gillen, K.T., Li, E.R.: Nuclear power plant cable materials - review of qualification and currently available aging data for margin assessments in cable performance. Sandia National Laboratories, Albuquerque, New Mexico (2013)
9. Barsoukov, E., Macdonald, J.R.: *Impedance Spectroscopy Theory, Experiment, and Applications*, 2nd edn. Wiley, Hoboken (2010)